

MIT Open Access Articles

*Thermal Conduction in Aligned Carbon Nanotube–
Polymer Nanocomposites with High Packing Density*

The MIT Faculty has made this article openly available. **Please share** how this access benefits you. Your story matters.

Citation: Marconnet, Amy M. et al. “Thermal Conduction in Aligned Carbon Nanotube–Polymer Nanocomposites with High Packing Density.” ACS Nano 5.6 (2011): 4818–4825. Web.

As Published: <http://pubs.acs.org/doi/abs/10.1021/nn200847u>

Publisher: American Chemical Society

Persistent URL: <http://hdl.handle.net/1721.1/71651>

Version: Author's final manuscript: final author's manuscript post peer review, without publisher's formatting or copy editing

Terms of Use: Article is made available in accordance with the publisher's policy and may be subject to US copyright law. Please refer to the publisher's site for terms of use.



Thermal Conduction in Aligned Carbon Nanotube- Polymer Nanocomposites with High Packing Density

Amy M. Marconnet,[†] Namiko Yamamoto,[‡] Matthew A. Panzer,[†]

Brian L. Wardle,[‡] and Kenneth E. Goodson^{†,}*

[†]Department of Mechanical Engineering, Bldg 530, Room 224, 440 Escondido Mall
Stanford University, Stanford, CA 94305

[‡]Department of Aeronautics and Astronautics, Room 41-317, 77 Mass. Ave.,
Massachusetts Institute of Technology, Cambridge, MA 02139

goodson@stanford.edu

RECEIVED DATE (to be automatically inserted after your manuscript is accepted if required according to the journal that you are submitting your paper to)

*Address correspondence to goodson@stanford.edu.

ABSTRACT

Nanostructured composites containing aligned carbon nanotubes (CNTs) are very promising as interface materials for electronic systems and thermoelectric power generators. We report the

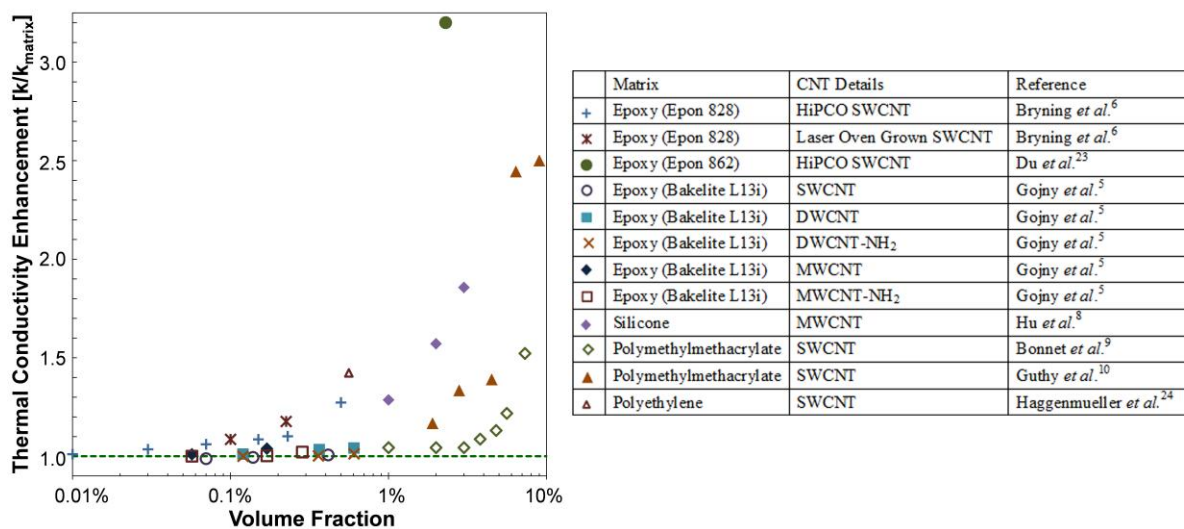
first data for thermal conductivity of densified, aligned multi-wall CNT nanocomposite films for a range of CNT volume fractions. A 1 *vol.%* CNT composite more than doubles the thermal conductivity of the base polymer. Denser arrays (17 *vol.%* CNTs) enhance the thermal conductivity by as much as a factor of 18 and there is a non-linear trend with CNT volume fraction. This article discusses the impact of CNT density on thermal conduction considering boundary resistances, increased defect concentrations, and the possibility of suppressed phonon modes in the CNTs.

Keywords: Carbon Nanotubes, Nanocomposites, Thermal Conductivity, Thermal Interface Materials

Aligned CNT polymer nanocomposites (A-CNT-PNCs) can benefit a variety of applications including electronics thermal management. Individual carbon nanotubes (CNTs) can have thermal conductivities near $3000 \text{ W m}^{-1} \text{ K}^{-1}$ and molecular dynamics simulations predict the values could be even higher.^{1, 2} Vertically aligned CNT films can have volume-averaged axial thermal conductivities as high as those of metals, with reported values reaching $\sim 265 \text{ W m}^{-1} \text{ K}^{-1}$.^{3, 4} However, pure CNT forests, without binding materials, do not always offer the mechanical properties required by structural, aerospace, and other applications. Recent progress on CNT-polymer composites, in particular those featuring aligned nanotubes, promises unique combinations of thermal and mechanical properties. We report here a detailed study of conduction along aligned CNT-epoxy composites with CNT volume fractions extending an order of magnitude higher (up to 20%) than those of previous research. In particular, this work finds that the axial thermal conductivity is increased by a factor of 18.5 at a volume fraction of 16.7

vol.%, and the observed conductivity anisotropy ($k_{\text{axial}}/k_{\text{transverse}} \sim 2$ to 5) correlates well with CNT alignment. A strongly nonlinear variation of axial conductivity with volume fraction is interpreted considering CNT-epoxy boundary resistances, CNT imperfections introduced during fabrication, and modification of the phonon conduction within the nanotubes due to interactions with the matrix (*e.g.* enhanced scattering, damping of phonon modes, *etc.*).

Carbon nanotube additives have yielded only modest increases in the thermal conductivities of polymers compared to theoretical predictions, and the reasons for the relatively low conductivities are not well understood. Figure 1 reviews prior data for composites containing randomly-oriented carbon nanotubes and polymers (thermal conductivities near $0.2 \text{ W m}^{-1} \text{ K}^{-1}$). Low concentrations of nanotubes ($<1 \text{ vol.}\%$) have been shown to reduce the effective composite thermal conductivity in some cases, possibly due to void formation, and yield a modest enhancement in others.⁵⁻⁷ Higher concentrations ($>1 \text{ vol.}\%$) yield larger increases in the conductivity, but generally less than twice the value of the epoxy matrix.^{5, 6, 8-10} The resulting nanotube composites have a much lower thermal conductivity than predicted by effective medium theory (EMT),^{11, 12} which, for example, predicts a factor of 250 enhancement in thermal conductivity when $5 \text{ vol.}\%$ randomly oriented CNTs ($k \sim 3000 \text{ W m}^{-1} \text{ K}^{-1}$) are added to an epoxy ($k_m \sim 0.2 \text{ W m}^{-1} \text{ K}^{-1}$). Possible reasons for the disparity between predictions and data include modification of the phonon conduction within the individual nanotubes by the polymer matrix,⁵ interfacial thermal resistances that impair thermal transport between the nanotubes and the polymer or between contacting nanotubes,^{7, 11-16} impurities and lattice defects within individual nanotubes,¹⁶⁻²⁰ and the formation of voids in the CNT-polymer composite.^{21, 22}



	Matrix	CNT Details	Reference
+	Epoxy (Epon 828)	HiPCO SWCNT	Bryning <i>et al.</i> ⁶
×	Epoxy (Epon 828)	Laser Oven Grown SWCNT	Bryning <i>et al.</i> ⁶
●	Epoxy (Epon 862)	HiPCO SWCNT	Du <i>et al.</i> ²³
○	Epoxy (Bakelite L13i)	SWCNT	Gojny <i>et al.</i> ⁵
■	Epoxy (Bakelite L13i)	DWCNT	Gojny <i>et al.</i> ⁵
×	Epoxy (Bakelite L13i)	DWCNT-NH ₂	Gojny <i>et al.</i> ⁵
◆	Epoxy (Bakelite L13i)	MWCNT	Gojny <i>et al.</i> ⁵
□	Epoxy (Bakelite L13i)	MWCNT-NH ₂	Gojny <i>et al.</i> ⁵
◇	Silicone	MWCNT	Hu <i>et al.</i> ⁸
◇	Polymethylmethacrylate	SWCNT	Bonnet <i>et al.</i> ⁹
▲	Polymethylmethacrylate	SWCNT	Guthy <i>et al.</i> ¹⁰
△	Polyethylene	SWCNT	Haggenmueller <i>et al.</i> ²⁴

Figure 1. Previous data for the thermal conductivity enhancement as a function of volume fraction for randomly dispersed CNT composites. This chart represents a subset of the available data where the matrix material has a thermal conductivity of 0.18 to 0.26 W m⁻¹ K⁻¹.

This work investigates the impact of CNT density on the thermal conductivity of nanocomposites consisting of mechanically-densified, aligned multi-walled CNT (MWCNT)

arrays infiltrated with an unmodified aerospace-grade thermoset epoxy. To better understand factors limiting thermal conductivity enhancement with the inclusion of nanotubes, both the axial and transverse thermal conductivities are compared with predictions from effective medium theory. The conduction mechanisms within the composites are considered to explain the observed non-linear increase in thermal conductivity with volume (packing) fraction of CNTs. Unlike unaligned, randomly-oriented nanotubes, aligned MWCNT arrays can potentially provide more direct thermal conductivity pathways across the entire composite thickness, which can yield significant thermal conductivity improvements.^{22, 25, 26} The present manuscript offers the first benchmark data of CNT composites with controlled CNT density allowing correlation between CNT density and composite thermal conductivity. These data complement previous work characterizing the mechanical and electrical properties of these mechanically densified aligned CNT composites (up to 20 *vol.*% CNTs), which showed promise for use in multifunctional applications with a factor of 3 enhancement in elastic modulus at 17 *vol.*% CNTs and a significant reduction in electrical resistance with increasing CNT density.^{27, 28}

MWCNT arrays are grown using chemical vapor deposition,²⁹ mechanically densified to increase the volume fraction,³⁰ and infiltrated with RTM6 epoxy. The CNT alignment within the composites is examined by measuring the azimuthal angle of CNTs using scanning electron microscopy (SEM, Philips XL30), resulting in a mean-square cosine of 0.77 from averaging over 100 CNTs. Voids in CNT composites are evaluated using optical microscopy and micro-computed tomography scans (X-Tek HMXST225), and only void-free A-CNT-PNC samples are thermally characterized.

Comparative infrared (IR) microscopy characterizes the axial and transverse thermal conductivities of aligned CNT nanocomposites of varying volume fraction. The measured

thermal conductivities (Figure 2) are comparable with or greater than those reported previously for other aligned CNT nanocomposites,^{22, 25} but the data fall well below the best data for CNT films without an epoxy matrix.^{3, 4, 31, 32} The axial thermal conductivity of the composites ranges from 0.46 to 4.87 W m⁻¹ K⁻¹ as the nanotube density increases from 1 vol.% to 16.7 vol.%. The axial thermal conductivity of the composites is comparable to the thermal conductivity of unfilled, aligned, densified MWCNT films which ranges from 0.29 to 3.6 W m⁻¹ K⁻¹ as shown in Figure 2. The unfilled arrays were fabricated in the same manner as the composites and measured with a similar comparative infrared microscopy technique as the composites with minor differences as noted in the Experimental section.

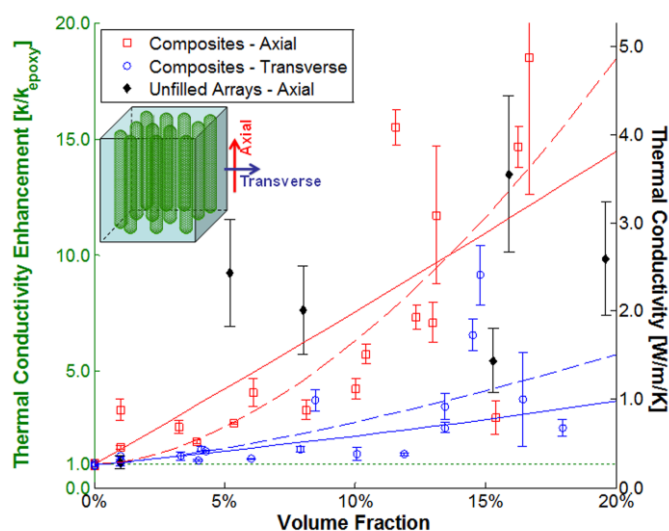


Figure 2. The axial (\square) and transverse (\circ) thermal conductivity of CNT nanocomposites and unfilled CNT forests (filled diamonds) as a function of volume fraction. The schematic below the legend shows the axial and transverse measurement directions for the aligned CNT composites. Best fits from the effective medium approach (solid lines) and with a power law (dashed line) are shown for the composite data. For the effective medium approach, the axial and transverse thermal conductivities are fit simultaneously with a non-linear least squares algorithm, assuming

an alignment factor of 0.77 from the SEM analysis, with two free parameters: the individual CNT thermal conductivity ($22.1 \text{ W m}^{-1} \text{ K}^{-1}$) and the CNT-polymer boundary resistance ($<1 \times 10^{-9} \text{ m}^2 \text{ K W}^{-1}$). For the power law relationship $(k_e - k_m) = A \cdot f^B$, the prefactor, A , and the exponent, B , are fit with a non-linear least squares algorithm, while the measured matrix thermal conductivity, $k_m = 0.26 \text{ W m}^{-1} \text{ K}^{-1}$, is held constant. The fitted values are $A = 72.9 \text{ W m}^{-1} \text{ K}^{-1}$ and $B = 1.72$ for the axial thermal conductivity and $A = 11.3 \text{ W m}^{-1} \text{ K}^{-1}$ and $B = 1.37$ for the transverse thermal conductivity. The dashed green line indicates the thermal conductivity of the epoxy.

RESULTS AND DISCUSSION

For the axial direction in the aligned composites, a simple model considering nanotubes conducting heat parallel with the polymer matrix predicts that the thermal conductivity increases linearly with volume fraction. A linear fit to the axial data in Figure 1 provides an estimate of $18.5 \text{ W m}^{-1} \text{ K}^{-1}$ for the thermal conductivity of the individual nanotubes in the matrix, much lower than the previous measurements of individual nanotubes. However, the axial thermal conductivity for the composites does not follow a simple linear trend, instead the increase in thermal conductivity with volume fractions above 10% appears much greater than at lower volume fractions suggesting that the density of nanotubes is not the only factor influencing the thermal conductivity. The non-linearity of the data in Figure 2 for the aligned CNT composites is similar to the data for the randomly-oriented composites presented in Figure 1, although the magnitude of the thermal conductivity enhancement is much greater for these aligned composites. The thermal conductivity for the transverse direction remains near the thermal conductivity of the base epoxy increasing slightly with volume fraction below $\sim 10 \text{ vol.}\%$. The highest measured transverse thermal conductivity is $2.41 \text{ W m}^{-1} \text{ K}^{-1}$ at $14.8 \text{ vol.}\%$. For both the

axial and transverse direction, at high volume fractions ($> 10 \text{ vol.}\%$), significant differences in the thermal conductivity are observed for samples of similar CNT densities indicating that variations in sample quality may impact the thermal conductivity. While isotropic thermal conductivity is expected and observed for randomly dispersed nanotube composites, the CNT alignment in these composites results in a significantly anisotropic thermal conductivity ($k_{\text{axial}}/k_{\text{transverse}} \sim 2$ to 5). The axial thermal conductivity increases more rapidly with volume fraction than the transverse thermal conductivity, resulting in a higher degree of anisotropy at higher volume fractions.

There are several possible explanations for the thermal conductivities reported here for composites, which are lower than expected for CNT-based materials and also lower than those reported for thin, unfilled and uncompressed CNT arrays. The same conduction mechanisms that reduce the thermal conductivity also dictate the non-linear trend in thermal conductivity with volume fraction. First, the quality of the CNT film used for composites strongly impacts the composite performance. Measurements and simulations of individual nanotubes highlight the very high thermal conductivities of pristine nanotubes leading to impressive predictions of the behavior of bulk materials fabricated from CNT films. But even for unfilled CNT arrays, the reported effective thermal conductivities range from less than $1 \text{ W m}^{-1} \text{ K}^{-1}$ (e.g. ³³) to over $250 \text{ W m}^{-1} \text{ K}^{-1}$ (e.g. ^{3, 4}). The effective thermal conductivity of the unfilled CNT arrays in this study, which form the basis of the composites used in this work ranges from 0.29 to $3.6 \text{ W m}^{-1} \text{ K}^{-1}$ over the range of volume fractions investigated. The low thermal conductivity for the unfilled arrays is governed by the quality of the CVD grown nanotubes and the challenge in making good thermal contact with all the nanotubes within the film. Thus, when filled with epoxy ($k \sim 0.26 \text{ W m}^{-1} \text{ K}^{-1}$ for the RTM6 used here), the composite thermal conductivity will not be as high as

predicted from the measurements of individual nanotubes. The effective thermal conductivity of bulk materials containing nanotubes depends on many properties of the CNT component, including the individual CNT conductivity, CNT density, morphology, and contact resistances. In particular, defects within individual nanotubes, including lattice defects, impurities, and amorphous carbon, lead to reduced thermal conductivities of the individual nanotubes, and hence of their bulk materials. Raman spectroscopy of MWCNT films is used to provide a very approximate indication of the impact of compression on quality. The ratio of the G (graphite) band to the D (defect) band in MWCNT films shows no detrimental effect of densification on quality of the MWCNT films at the maximum compression (20 vol % MWCNTs).³⁴ Improvements in thermal conductivity for CNT films and composites have been observed after various treatments such as annealing,^{19, 20} nitric acid treatments,^{18, 19} and centrifugation (for unaligned films).¹⁷ In order to form high thermal conductivity composites, the thermal conductivity of the constituent CNTs must be consistently high, and this is not always achieved in the quantities needed for fabricating nanocomposites.

Second, contact regions between nanotubes, which occur even in the best aligned CNT films, impact thermal performance of any CNT composite. These contact points serve both as scattering sites for phonons propagating along contacting nanotubes, reducing the individual nanotube thermal conductivity, and as a route for heat conduction between the nanotubes with additional thermal resistance across the interface. The magnitude of the thermal boundary resistance at CNT-CNT contacts strongly influences the effective conductivity of the composite material. A higher contact resistance diminishes the thermal conductivity of the ensemble. Prasher *et al.*¹⁵ show that the thermal conductivity of a randomly-oriented bed of MWCNTs is controlled by the CNT-CNT thermal contact resistance which is orders of magnitude larger than

the intrinsic thermal resistance of a CNT. If the thermal boundary resistance between nanotubes is small, as the volume fraction increases and more CNT-CNT contacts are formed, the composite thermal conductivity increases. Percolation theory predicts that above a threshold volume fraction, the filler particles (CNTs) form a network which bridges the entire thickness of the composite leading to more effective heat transport across a sample.^{8, 13} Kumar *et al.*¹³ computationally analyzed percolation in 2D networks of CNTs, finding that the CNT-CNT and CNT-substrate thermal resistances influenced the thermal conductivity, even below the threshold volume fraction required to form chains of filler CNTs bridging the entire sample thickness. In contrast, in the axial direction, the nanotubes in the composites studied in this work should bridge the entire thickness of the sample in the axial direction regardless of the volume fraction. But in the transverse direction and in the axial direction if some CNTs do not traverse the entire sample thickness, densification may lead to the formation of percolation networks which bridge the entire thickness of the sample. Meshot and Hart³⁵ have shown variations in CNT alignment and entanglement from the top to bottom of similar CVD grown MWCNT arrays. Panzer *et al.*³⁶ showed that not all nanotubes physically present in a aligned array contribute to heat transport due to a lack of engagement of all the CNTs with the heat source and sink. As the alignment and continuity of the nanotubes varies throughout the array, CNT-CNT contacts become increasingly important for effective heat transport across the composite.

Third, CNT-polymer boundary resistance impacts the effective thermal conductivity of CNT-polymer composites. In unaligned CNT composites, the individual CNTs do not bridge the entire thickness of the composite and the CNT-polymer boundary resistance is critical. One of the main advantages of the composites studied in this work is that the CNTs themselves are well-aligned and span the entire thickness of the polymer in the axial direction providing direct pathways for

heat transport across the composite. In theory, for these composites, the CNT-polymer boundary resistance is only important for the conductivity transverse to the CNT axis. However, if some of the CNTs fail to extend to the surface of the polymer, the CNT-polymer thermal boundary resistance will impact the axial conduction as well.

Furthermore, phonon modes within CNTs can be damped and scattered by the polymer matrix reducing the thermal conductivity of the CNTs themselves.^{5, 7} Gojny *et al.*⁵ showed that the thermal conductivity enhancement for MWCNTs dispersed in epoxy was larger than that of single-walled CNTs (SWCNTs) as MWCNTs have inner shells which conduct phonons efficiently despite the outer shell interacting with the polymer matrix. This damping of phonon modes within the outer shells of nanotube may be a possible reason for the reduction of the thermal conductivity of the nanotubes, especially when high quality nanotubes form the basis of the composite.

The effect of CNT-CNT contacts is the most likely cause of the non-linearity in the thermal conductivity with increased density, while the low thermal conductivity of the constituent CNT arrays dictates the low thermal conductivity compared to pristine nanotubes. The number of contact points and the area of each contact could be affected by the biaxial compression and by the addition of epoxy to the composite. Increasing area of contact should reduce the contact resistance, while increasing contacts may lead to increased scattering but more opportunities for heat to transfer between neighboring nanotubes. The CNT-polymer boundary resistance may also contribute to the non-linearity of the thermal conductivity with increased density, particularly in the direction transverse to the CNT axis. All nanotubes in this work are grown following the same procedure, so the CNT array quality should be consistent even at high volume fractions. The scatter in the data for unfilled arrays may arise from variations in the quality of thermal

contact to the substrate after densification. Poor contact between the substrate and the nanotubes, combined with minimal conduction between nanotubes, may lead to few pathways for thermal conduction across the CNT array. For PNCs, the matrix can aid in spreading the heat between nanotubes, especially at the contact surfaces.

Effective medium theory¹² has been used to model the thermal conductivity of CNT-polymer composites in the axial and transverse directions. The CNT-polymer boundary resistance dictates the curvature of the transverse thermal conductivity with increased CNT volume fractions. Relatively small values of CNT-polymer boundary resistance ($<1 \times 10^{-9} \text{ m}^2 \text{ K W}^{-1}$) are required to see the positive curvature observed with these experiments. When fitting effective medium theory to the data, little non-linearity in the EMT prediction is observed, as seen in Figure 2. The generally aligned, but wavy, entangled, cylindrical CNTs are modeled as unaligned ellipsoidal particles with a large aspect ratio. The alignment factor, $\langle \cos^2(\theta) \rangle$, varies from 0.33 for completely randomly oriented particles to 1 for particles whose axis aligns perfectly (i.e., collimated) with the direction of heat transport. Fitting both the axial and transverse thermal conductivity data predicts an individual CNT thermal conductivity of $22.1 \text{ W m}^{-1} \text{ K}^{-1}$ and a boundary resistance $<1 \times 10^{-9} \text{ m}^2 \text{ K W}^{-1}$, assuming an alignment factor of 0.77 from the SEM analysis. This EMT model incorporates the thermal boundary resistance between the CNT and the polymer, R_{bd} , but neglects direct CNT-CNT conduction. Considering the axial direction, the model elliptical particle may represent a heat transfer pathway consisting of more than one nanotube, in which case, the effective thermal conductivity predicted includes the intrinsic thermal conductivity and thermal boundary resistances and requires a low value of the intrinsic CNT thermal conductivity to achieve agreement with the data. Furthermore, by neglecting the direct CNT-CNT conduction, this model may also underpredict the CNT-epoxy boundary

resistances. This may account for the disparity between our estimate of CNT-epoxy boundary resistance and values on the order of 10^{-8} to 10^{-7} $\text{m}^2 \text{K} / \text{W}$ reported in literature.^{37, 38}

Fitting a power law relationship, similar to the results of percolation theory, to the increase in the axial thermal conductivity above the polymer matrix gives a better approximation of the

trend in the data leading to the relation $(k_{e,a} - k_m) = \left(72.9 \frac{\text{W}}{\text{m} \cdot \text{K}}\right) f^{1.72}$. The fit to the transverse conductivity leads to a different exponential relationship with a slightly lower exponent:

$(k_{e,t} - k_m) = \left(11.3 \frac{\text{W}}{\text{m} \cdot \text{K}}\right) f^{1.37}$. The power law relation suggests that there are an increasing number of pathways for heat transport generated by increasing volume fraction.

In conclusion, the first benchmark study of the thermal conductivity of aligned MWCNT polymer nanocomposites as a function of varying CNT volume fraction is reported. Axial thermal conductivities up to $4.87 \text{ W m}^{-1} \text{ K}^{-1}$ with 16.7 vol.% CNTs (a factor of 18.5 enhancement in thermal conductivity) are reported for the axial direction, much greater than reported in studies of unaligned CNT composites. While the thermal conductivity enhancement is large, it is much lower than predicted if the thermal conductivity of the individual, defect-free CNTs have thermal conductivities on the order of $3000 \text{ W m}^{-1} \text{ K}^{-1}$, but it is comparable to the thermal conductivity of the unfilled CNT arrays. The non-linear behavior of thermal conductivity with CNT volume fraction is attributed to the interaction between CNTs and between the CNT and the polymer. Future measurements of the transverse conductivity of unfilled arrays will be useful in separating out the effects of the epoxy infiltration from the effects of CNT-CNT interactions. Further model development is necessary to fully understand the impact of factors including CNT waviness, boundary resistances, and parameter variation with CNT volume fraction. In order to fabricate composites that take full advantage of the high thermal conductivity of individual CNTs,

additional studies on aligned CNT composites are necessary including improvement of the CNT quality (through post-growth annealing processes, *etc.*) and improved epoxy infiltration to minimize CNT-CNT contacts. In addition to thermal properties, the composites also need to be engineered to obtain the desired mechanical properties for thermal interface applications.

METHODS

Fabrication: Aligned CNT composites are fabricated from continuous CNTs, implemented in a controlled and aligned morphology as described in previous work^{27, 30} and illustrated in Figure 3. In brief, aligned arrays consisting of 1 *vol.*% dense, 8 nm diameter, several millimeter long MWCNTs are grown *via* chemical vapor deposition. The aligned arrays are densified using biaxial mechanical compression and infiltrated using capillary action with epoxy (RTM6 from Hexcel), then cured to form aligned CNT nanocomposites with CNT densities between 1 *vol.*% and 20 *vol.*%. The CNT alignment was quantified by measuring the azimuthal angle θ of CNTs using scanning electron microscopy (SEM, Philips XL30). The mean-square cosine $\langle \cos^2 \theta \rangle$, with its statistical distribution among all CNTs as the weighting factor, was estimated to be 0.77 from averaging over 100 CNTs in the SEM images. Voids in CNT composites were also evaluated using optical microscopy (2D) and micro-computed tomography scan (X-Tek HMXST225, 3D). Air bubbles and epoxy-rich regions on the order of microns were at times observed and A-CNT-PNC samples with such voids were eliminated from the sample sets.³⁴

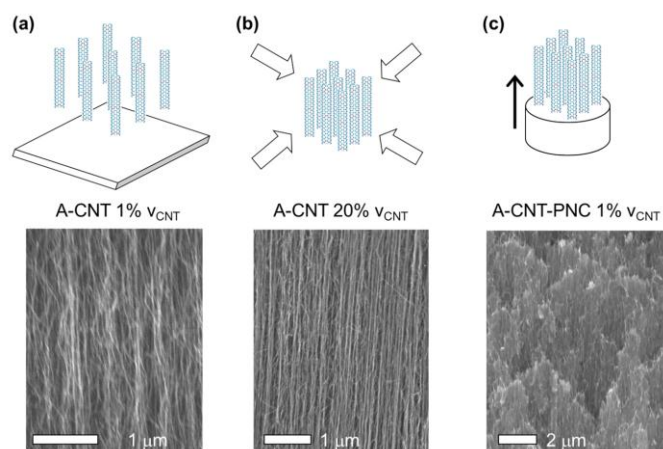


Figure 3. Schematic and SEMs of nanocomposite fabrication.^{27, 30} (a) As grown CNT films with 1 vol.% CNTs. (b) Biaxial mechanical compression of CNTs up to 20 vol.% CNTs. (c) A-CNT-PNC fracture surface after capillary-driven epoxy infiltration of the CNT arrays.

Comparative Infrared Thermal Microscopy: The thermal conductivity is measured using a comparative method based on ASTM standard E1225, using an infrared (IR) microscope instead of thermocouples.³⁹⁻⁴¹ A one-dimensional heat flux is generated across a stack consisting of the nanocomposite sample sandwiched between two reference layers. A resistive heater (metal-coated silicon) is attached to one reference layer, and the other reference layer is affixed to a heat sink (through a silicon wafer attached to temperature-controlled copper baseplate). For the unfilled CNT arrays, the stack consists only of a heat sink (silicon wafer attached to copper baseplate), a reference layer, a sample CNT film, and a heater (metal-coated silicon). Based on preliminary work regarding the magnitude of the thermal conductivity, one of two reference materials are used for each samples in this experiment: quartz (GE Type 214) with a thermal conductivity of $1.4 \text{ W m}^{-1} \text{ K}^{-1}$ and Pyrocera 9606 (Corning Glass) with a thermal conductivity of $4 \text{ W m}^{-1} \text{ K}^{-1}$, to ensure that the temperature gradients in the sample and in the reference layers are comparable.

Fourier's law describes heat transport for each layer in the sample. The samples are prepared such that all layers in the stack have the same cross-section and the heat flux is constant across the sample and two reference layers. Thus, the ratio of the thermal conductivity of the sample and the reference material can be determined from a ratio of the temperature gradient in the sample and the reference layer. The use of two reference layers allows the relative importance of any other heat transfer mechanisms, such as convective and radiative loss, compared to the conduction through the sample stack to be determined. Also, the use of reference layers eliminates possible error due to electrical losses in the wiring and connections supplying power to the heater and due to convection to the air on the topside of the heater. The relevant surfaces of the composite which come in contact with the reference layers are polished to a roughness of less than 3 nm and coated with 200 nm of platinum to enhance contact. The sample stack is assembled using a silver epoxy (Duralco 120, Cortonics). The surfaces of the reference-sample-reference stack facing the IR camera view are also polished, and then coated with a thin film of carbon (SPRAYON Dry Graphite Lubricant, Sherwin Williams) to enhance emissivity. For the unfilled CNT arrays, no surfaces are polished or coated with platinum and the stack is bonded together using colloidal graphite (Ted Pella, Inc.) and the surfaces of the reference layer are also coated with the colloidal graphite to enhance emissivity.

For a given heater power, a two-dimensional temperature map is recorded with the infrared microscope. The microscope uses a 256x256 InSb focal plane array for detecting wavelengths ranging from 3 to 5 μm . The IR microscope has a temperature sensitivity of 0.1 K and spatial resolution of up to 2 μm . Within each temperature map, the regions containing the reference layers and sample are identified and the temperature is averaged in the direction perpendicular to the heat transport to yield temperature versus position graphs, as shown in Figure 4. The

temperature gradient in each region of the stack is determined using a least-squares fitting routine. For a robust measurement, thermal maps are recorded and the thermal gradients are calculated as the power is increased. Boundary resistances between the different layers in the stack can be spatially separated from the temperature gradients associated with the material's intrinsic thermal conductivity.

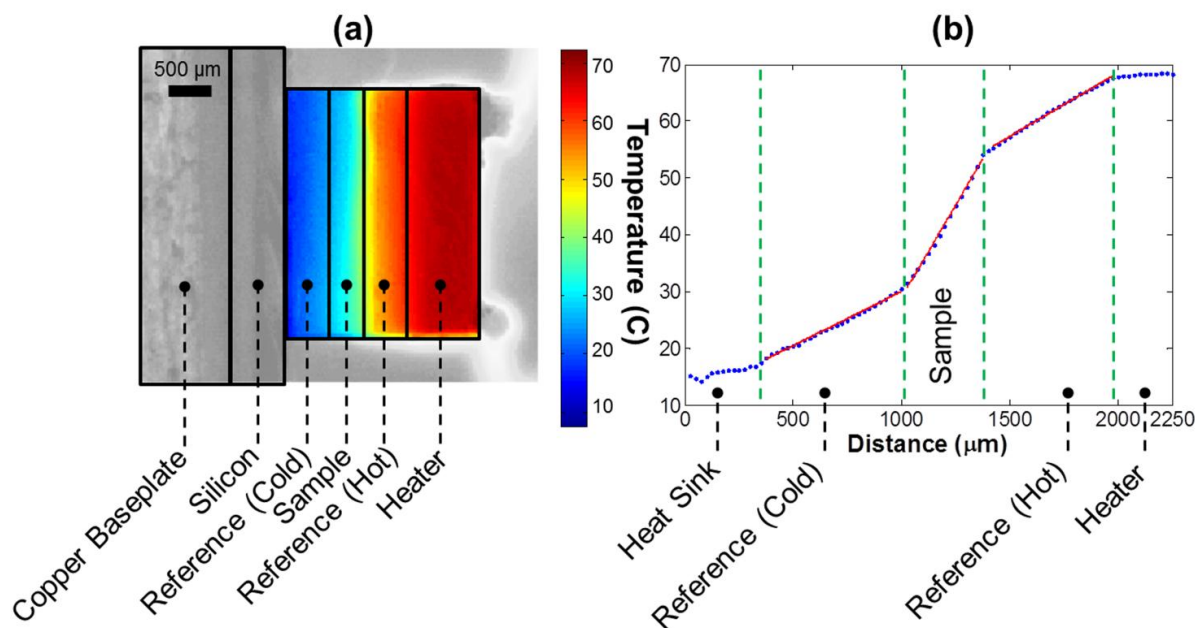


Figure 4. IR Microscopy technique for thermal conductivity measurements. (a) Schematic of the testing configuration with an example temperature map. The sample sandwiched between two reference layers. A metallized piece of silicon is used as a heater and the structure is affixed to a silicon substrate with silver paste. The silicon substrate is affixed to the temperature controlled copper baseplate using thermal grease. (b): Temperature distribution across sample including best fit slopes for both reference regions and the sample (temperatures averaged across the width of sample, *i.e.* each column in image (a)).

ACKNOWLEDGMENT

The authors gratefully acknowledge the financial support from the ONR (N00014-09-1-0296-P00004, Dr. Mark Spector – program manager), the NSF-DOE thermoelectrics partnership (CBET0853350), the National Science Foundation Graduate Research Fellowship program, and the Stanford Graduate Fellowship program. This work was supported also by Airbus S.A.S., Boeing, Embraer, Hexcel, Lockheed Martin, Saab AB, Spirit AeroSystems, Textron Inc., Composite Systems Technology, and TohoTenax through MIT's Nano-Engineered Composite aerospace STructures (NECST) Consortium. Namiko Yamamoto acknowledges the Linda and Richard (1958) Hardy Fellowship. This work made use of the Shared Experimental Facilities supported in part by the MRSEC Program of the National Science Foundation under award number DMR-0819762.

REFERENCES

1. Kim, P.; Shi, L.; Majumdar, A.; McEuen, P. L. Thermal Transport Measurements of Individual Multiwalled Nanotubes. *Phys. Rev. Lett.* **2001**, *87*, 215502.
2. Berber, S.; Kwon, Y.-K.; Tománek, D., Unusually High Thermal Conductivity of Carbon Nanotubes. *Phys. Rev. Lett.* **2000**, *84*, 4613.
3. Tong, T.; Majumdar, A.; Yang, Z.; Kashani, A.; Delzeit, L.; Meyyappan, M. Indium Assisted Multiwalled Carbon Nanotube Array Thermal Interface Materials. In *10th Intersoc. Conf. Therm. Thermomech. Phenom. Electron. Syst.*, San Diego, CA, May 30 - June 2, 2006; pp 1406-1411.
4. Tong, T.; Yang, Z.; Delzeit, L.; Kashani, A.; Meyyappan, M.; Majumdar, A., Dense Vertically Aligned Multiwalled Carbon Nanotube Arrays as Thermal Interface Materials. *IEEE Trans. Compon. Packag. Technol.* **2007**, *30*, 92-100.
5. Gojny, F. H.; Wichmann, M. H. G.; Fiedler, B.; Kinloch, I. A.; Bauhofer, W.; Windle, A. H.; Schulte, K., Evaluation and Identification of Electrical and Thermal Conduction Mechanisms in Carbon Nanotube/Epoxy Composites. *Polymer* **2006**, *47*, 2036-2045.
6. Bryning, M. B.; Milkie, D. E.; Islam, M. F.; Kikkawa, J. M.; Yodh, A. G. Thermal Conductivity and Interfacial Resistance in Single-Wall Carbon Nanotube Epoxy Composites. *Appl. Phys. Lett.* **2005**, *87*, 161909-3.
7. Mamunya, Y.; Boudenne, A.; Lebovka, N.; Ibois, L.; Candau, Y.; Lisunova, M. Electrical and Thermophysical Behaviour of Pvc-Mwcnt Nanocomposites. *Compos. Sci. Technol.* **2008**, *68*, 1981-1988.

8. Hu, X.; Jiang, L.; Goodson, K. E. Thermal Conductance Enhancement of Particle-Filled Thermal Interface Materials Using Carbon Nanotube Inclusions, In *9th Intersoc. Conf. Therm. Thermomech. Phenom. Electron. Syst.*, Las Vegas, NV, June 1-4, 2004; pp 63-69.
9. Bonnet, P.; Sireude, D.; Garnier, B.; Chauvet, O. Thermal Properties and Percolation in Carbon Nanotube-Polymer Composites. *Appl. Phys. Lett.* **2007**, *91*, 201910-3.
10. Guthy, C.; Du, F.; Brand, S.; Winey, K. I.; Fischer, J. E. Thermal Conductivity of Single-Walled Carbon Nanotube/Pmma Nanocomposites. *J. Heat Transfer* **2007**, *129*, 1096-1099.
11. Nan, C. W.; Shi, Z.; Lin, Y. A Simple Model for Thermal Conductivity of Carbon Nanotube-Based Composites. *Chem. Phys. Lett.* **2003**, *375*, 666-669.
12. Nan, C.-W.; Birringer, R.; Clarke, D. R.; Gleiter, H. Effective Thermal Conductivity of Particulate Composites with Interfacial Thermal Resistance. *J. Appl. Phys.* **1997**, *81*, 6692-6699.
13. Kumar, S.; Alam, M. A.; Murthy, J. Y. Effect of Percolation on Thermal Transport in Nanotube Composites. *Appl. Phys. Lett.* **2007**, *90*, 104105-3.
14. Nan, C.-W.; Liu, G.; Lin, Y.; Li, M. Interface Effect on Thermal Conductivity of Carbon Nanotube Composites. *Appl. Phys. Lett.* **2004**, *85*, 3549-3551.
15. Prasher, R. S.; Hu, X. J.; Chalopin, Y.; Mingo, N.; Lofgreen, K.; Volz, S.; Cleri, F.; Koblinski, P. Turning Carbon Nanotubes from Exceptional Heat Conductors into Insulators. *Phys. Rev. Lett.* **2009**, *102*, 105901-4.
16. Borca-Tasciuc, T.; Borca-Tasciuc, D. A.; Gang, C. A Photo-Thermoelectric Technique for Anisotropic Thermal Diffusivity Characterization of Nanowire/Nanotube Composites. In *Annual IEEE Semicond. Therm. Meas. Manage. Symp.*, San Jose, CA, March 15-17, 2005; pp 283-291.
17. Yu, A.; Itkis, M. E.; Bekyarova, E.; Haddon, R. C. Effect of Single-Walled Carbon Nanotube Purity on the Thermal Conductivity of Carbon Nanotube-Based Composites. *Appl. Phys. Lett.* **2006**, *89*, 133102-3.
18. Hu, H.; Yu, A.; Kim, E.; Zhao, B.; Itkis, M. E.; Bekyarova, E.; Haddon, R. C. Influence of the Zeta Potential on the Dispersability and Purification of Single-Walled Carbon Nanotubes. *J. Phys. Chem. B* **2005**, *109*, 11520-11524.
19. Liu, C. H.; Fan, S. S. Effects of Chemical Modifications on the Thermal Conductivity of Carbon Nanotube Composites. *Appl. Phys. Lett.* **2005**, *86*, 123106-3.
20. Ivanov, I.; Puretzky, A.; Eres, G.; Wang, H.; Pan, Z.; Cui, H.; Jin, R.; Howe, J.; Geoghegan, D. B. Fast and Highly Anisotropic Thermal Transport through Vertically Aligned Carbon Nanotube Arrays. *Appl. Phys. Lett.* **2006**, *89*, 223110-3.
21. Grunlan, J. C.; Kim, Y. S.; Ziaee, S.; Wei, X.; Abdel-Magid, B.; Tao, K. Thermal and Mechanical Behavior of Carbon-Nanotube-Filled Latex. *Macromol. Mater. Eng.* **2006**, *291*, 1035-1043.
22. Borca-Tasciuc, T.; Mazumder, M.; Son, Y.; Pal, S. K.; Schadler, L. S.; Ajayan, P. M. Anisotropic Thermal Diffusivity Characterization of Aligned Carbon Nanotube-Polymer Composites. *J. Nanosci. Nanotechnol.* **2007**, *7*, 1581-1588.
23. Du, F.; Guthy, C.; Kashiwagi, T.; Fischer, J. E.; Winey, K. I. An Infiltration Method for Preparing Single-Wall Nanotube/Epoxy Composites with Improved Thermal Conductivity. *J. Polym. Sci., Part B: Polym. Phys.* **2006**, *44*, 1513-1519.
24. Hagenmueller, R.; Guthy, C.; Lukes, J. R.; Fischer, J. E.; Winey, K. I. Single Wall Carbon Nanotube/Polyethylene Nanocomposites: Thermal and Electrical Conductivity. *Macromolecules* **2007**, *40*, 2417-2421.

25. Huang, H.; Liu, C. H.; Wu, Y.; Fan, S. Aligned Carbon Nanotube Composite Films for Thermal Management. *Adv. Mater.* **2005**, *17*, 1652-1656.
26. Wu, Y.; Liu, C. H.; Huang, H.; Fan, S. Effects of Surface Metal Layer on the Thermal Contact Resistance of Carbon Nanotube Arrays. *Appl. Phys. Lett.* **2005**, *87*, 213108-3.
27. Garcia, E. J.; Saito, D. S.; Megalini, L.; Hart, A. J.; Villoria, R. G. d.; Wardle, B. L. Fabrication and Multifunctional Properties of High Volume Fraction Aligned Carbon Nanotube Thermoset Composites. *J. Nano Syst. Technol.* **2009**, *1*, 1-11.
28. Cebeci, H.; Villoria, R. G. d.; Hart, A. J.; Wardle, B. L. Multifunctional Properties of High Volume Fraction Aligned Carbon Nanotube Polymer Composites with Controlled Morphology. *Compos. Sci. Technol.* **2009**, *69*, 2649-2656.
29. Hart, A. J.; Slocum, A. H. Rapid Growth and Flow-Mediated Nucleation of Millimeter-Scale Aligned Carbon Nanotube Structures from a Thin-Film Catalyst. *J. Phys. Chem. B* **2006**, *110*, 8250-8257.
30. Wardle, B. L.; Saito, D. S.; García, E. J.; Hart, A. J.; de Villoria, R. G.; Verploegen, E. A. Fabrication and Characterization of Ultrahigh-Volume- Fraction Aligned Carbon Nanotube–Polymer Composites. *Adv. Mater.* **2008**, *20*, 2707-2714.
31. Cola, B. A.; Xu, X.; Fisher, T. S. Increased Real Contact in Thermal Interfaces: A Carbon Nanotube/Foil Material. *Appl. Phys. Lett.* **2007**, *90*, 093513-3.
32. Panzer, M. A.; Zhang, G.; Mann, D.; Hu, X.; Pop, E.; Dai, H.; Goodson, K. E. Thermal Properties of Metal-Coated Vertically Aligned Single-Wall Nanotube Arrays. *J. Heat Transfer* **2008**, *130*, 052401-9.
33. Wang, X.; Zhong, Z.; Xu, J. Noncontact Thermal Characterization of Multiwall Carbon Nanotubes. *J. Appl. Phys.* **2005**, *97*, 064302-5.
34. Yamamoto, N. Multi-Scale Electrical and Thermal Properties of Aligned Multi-Walled Carbon Nanotubes and Their Composites. Massachusetts Institute of technology, Cambridge, MA, 2011.
35. Meshot, E. R.; Hart, A. J. Abrupt Self-Termination of Vertically Aligned Carbon Nanotube Growth. *Appl. Phys. Lett.* **2008**, *92*, 113107-3.
36. Panzer, M. A.; Duong, H. M.; Okawa, J.; Shiomi, J.; Wardle, B. L.; Maruyama, S.; Goodson, K. E. Temperature-Dependent Phonon Conduction and Nanotube Engagement in Metalized Single Wall Carbon Nanotube Films. *Nano Lett.* **2010**, *10*, 2395-2400.
37. Huxtable, S. T.; Cahill, D. G.; Shenogin, S.; Xue, L.; Ozisik, R.; Barone, P.; Usrey, M.; Strano, M. S.; Siddons, G.; Shim, M.; Keblinski, P. Interfacial Heat Flow in Carbon Nanotube Suspensions. *Nat. Mater.* **2003**, *2*, 731-734.
38. Clancy, T. C.; Frankland, S. J. V.; Hinkley, J. A.; Gates, T. S. Multiscale Modeling of Thermal Conductivity of Polymer/Carbon Nanocomposites. *Int. J. Therm. Sci.* **2010**, *49*, 1555-1560.
39. Hu, X. J.; Panzer, M. A.; Goodson, K. E. Infrared Microscopy Thermal Characterization of Opposing Carbon Nanotube Arrays. *J. Heat Transfer* **2007**, *129*, 91.
40. Duong, H.; Yamamoto, N.; Panzer, M.; Marconnet, A.; Goodson, K. E.; Papavassiliou, D.; Maruyama, S.; Wardle, B. Thermal Properties of Vertically Aligned Carbon Nanotube-Nanocomposites Boundary Resistance and Inter- Carbon Nanotube Contact: Experiments and Modeling. In *APS Meeting 2009*, Pittsburgh, PA, March 16-20, 2009.
41. Marconnet, A.; Yamamoto, N.; Panzer, M.; Duong, H.; Wardle, B.; Goodson, K. E. Thermal Conductivity and Boundary Resistance of Aligned Carbon Nanotube Films and Their Polymeric Composites. In *Mater. Res. Soc. Symp. Proc.*, San Francisco, CA, April 13-17, 2009.

SYNOPSIS TOC

